Computer Modeling in Engineering & Sciences

Tech Science Press

DOI: 10.32604/cmes.2024.049124

ARTICLE

Dynamic Characteristics of Functionally Graded Timoshenko Beams by Improved Differential Quadrature Method

Xiaojun Huang[1], Liaojun Zhang[2,*], Hanbo Cui[1] and Gaoxing Hu[1]

[1]School of Architecture and Civil Engineering, Anhui Polytechnic University, Wuhu, 241000, China

[2]College of Water Conservancy and Hydropower Engineering, Hohai University, Nanjing, 210098, China

*Corresponding Author: Liaojun Zhang. Email: hohaihuang163@163.com

Received: 28 December 2023 Accepted: 06 March 2024 Published: 20 May 2024

ABSTRACT

This study proposes an effective method to enhance the accuracy of the Differential Quadrature Method (DQM) for calculating the dynamic characteristics of functionally graded beams by improving the form of discrete node distribution. Firstly, based on the first-order shear deformation theory, the governing equation of free vibration of a functionally graded beam is transformed into the eigenvalue problem of ordinary differential equations with respect to beam axial displacement, transverse displacement, and cross-sectional rotation angle by considering the effects of shear deformation and rotational inertia of the beam cross-section. Then, ignoring the shear deformation of the beam section and only considering the effect of the rotational inertia of the section, the governing equation of the beam is transformed into the eigenvalue problem of ordinary differential equations with respect to beam transverse displacement. Based on the differential quadrature method theory, the eigenvalue problem of ordinary differential equations is transformed into the eigenvalue problem of standard generalized algebraic equations. Finally, the first several natural frequencies of the beam can be calculated. The feasibility and accuracy of the improved DQM are verified using the finite element method (FEM) and combined with the results of relevant literature.

KEYWORDS

Timoshenko beams; functionally graded materials; dynamic characteristics; natural frequency; improved differential quadrature method

1 Introduction

Functionally graded materials (FGMs) are a new kind of material whose physical properties gradually change in one or more directions. This continuity of material properties overcomes many shortcomings of bonded materials. After several years of development, the application of functionally graded materials has expanded from the initial aeronautical field to the engineering field, such as nuclear power engineering, civil engineering, and others. The dynamic characteristics of functionally graded beams have always concerned scholars. Generally, establishing physical models that accurately reflect the laws of mechanics and the solution of corresponding mathematical equations are two critical steps in analyzing engineering structures. Due to the nonlinearity of the material properties of functionally graded beams, it is difficult to obtain analytical solutions for the dynamic governing

equations of such structures. Therefore, numerical methods have become commonly used for solving mathematical equations.

Many studies have been devoted to the dynamic characteristics of functionally graded beams. Kirlangic et al. [1] studied the dynamic characteristics of composite and functionally graded beams using the Ritz and Newmark average acceleration methods. Shang Hsu [2] presented a free vibration analysis of Timoshenko beam models using enriched finite element approaches. A two-node element was suggested by Moallemi-Oreh et al. [3] to analyze the stability and free vibration of Timoshenko beams. Tests showed high accuracy of the element in analyzing beams' stability and finding its critical load and free vibration analysis. Xu et al. [4] performed the free vibration analysis of Timoshenko beams with various combinations of boundary conditions by using the discrete singular convolution (DSC). For the free vibration of functionally graded beams whose physical properties changed along the axis due to the elastic modulus, shear modulus, and density of axially functionally graded materials changing continuously along the axis, the study of the free vibration of beams was complicated [5–7]. For the free vibration and stability of functionally graded beams with material properties varying along the thickness direction, Sankar [8] assumed that Young's modulus of the beam varied exponentially through the thickness. An elasticity solution was obtained for a functionally graded beam under transverse loads. Pu et al. [9] investigated the bending characteristics of functionally graded sandwich beams using an improved Fourier method under classical and non-classical boundary conditions. By comparing the results with other numerical methods, it was verified that the formula had high convergence speed and accuracy, but the derivation of the formula was complex. Stojanovic et al. [10] investigated the stability of uniform motion of multiple oscillators along a shear deformation beam on a viscoelastic foundation. The fully stable region is determined and discussed according to the change in the number of oscillators. Stojanovic et al. [11] studied the effects of the parameters of the laminate, the damping coefficient, and the spectral density on the random stability of the composite laminate. Qian et al. [12] studied the static deformations free and forced vibrations of FGMs cantilever beam by the Meshless Local Petrov-Galerkin (MLPG) method. Xiang et al. [13] investigated the free and forced vibration of a laminated functionally graded beam of variable thickness within the framework of Timoshenko beam theory. Gao et al. [14–16] used the two-step perturbation method to solve the nonlinear vibration governing equation, and the free vibration problem of beams with different functionally graded distributions is studied. Stojanovic et al. [17] investigated the coupled vibration and stability of multiple rectangular plates; the analytical solutions for the natural frequencies and critical buckling loads of the plates were obtained. Zheng et al. [18] proposed a general two-dimensional solution for cantilever FGMs beams under the Airy stress function. Huang et al. [19,20] developed methods to solve the natural frequency and vibration modal functions of functionally graded beams using the differential quadrature method. Choe et al. [21,22] studied the free vibration characteristics of functionally graded beams with arbitrary boundary conditions using numerical and semi-analytical methods.

Based on the literature review, there have been many studies on the vibration characteristics of beams with different gradient distributions, and numerous numerical calculation methods have also been proposed. However, they all suffer from the disadvantages of complex calculation processes and difficult programming solutions. The differential quadrature method (DQM) is a widely employed numerical technique for analyzing nonlinear structures owing to its straightforward solution process, uncomplicated programming, and superior computational efficiency. The precision of the calculation results of the method mainly depends on the discrete form of the nodes. This study modifies the discrete form of the conventional differential quadrature method. A discrete form of distribution of points in a proportional series is proposed, and the step size of nodes is adjusted by changing the

common ratio to control the precision of numerical calculation. Thus, the dynamic characteristics of FGMs beams along the thickness direction are investigated using the improved DQM. Firstly, based on the first-order shear deformation theory, the governing equation of transverse free vibration of a Timoshenko beam is transformed into the eigenvalue problem of ordinary differential equations. Then, the differential quadrature method is applied to transform the eigenvalue problem of the derived differential equation into the eigenvalue problem of standard generalized algebraic equations. Finally, the first several natural frequencies of transverse free vibration of the FGMs beam can be calculated by the QR method at one time. The method is verified by literature comparison and the mature numerical calculation method, which showed the applicability and high efficiency of the proposed method for solving variable differential equations.

2 Theoretical Formulations and Calculation Method

2.1 Beam Theory of Considering the Effects of Shear Deformation and Rotational Inertia of the Cross-Section

Consider a Timoshenko beam made of ceramic-metal materials in this section. The beam's length was denoted as L, width as b, and height as h, with a rectangular coordinate system o(x,y,z) assumed such that the x-axis was considered the neutral axis of a Timoshenko beam, the positive z-axis was directed upward and perpendicular to the x-axis, and the origin was located at the centroid of the rectangular section as shown in Fig. 1.

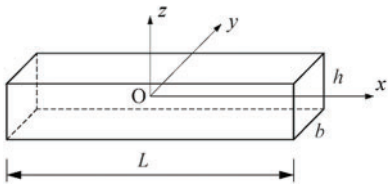

Figure 1: Schematic diagram of a beam with a gradient along the thickness direction

It was proposed that the parameters of the functionally graded materials adopt the linear mixing rate model. Hence, the elastic modulus $E(z)$ and density $\rho(z)$ were assumed to follow power-law functions in the thickness as Eq. (1).

$$\begin{cases} E(z) = E_m + (E_c - E_m)\left(\dfrac{1}{2} - \dfrac{z}{h}\right)^p \\ \rho(z) = \rho_m + (\rho_c - \rho_m)\left(\dfrac{1}{2} - \dfrac{z}{h}\right)^p \end{cases} \tag{1}$$

where E_c and E_m are the elastic modulus of ceramic and metal materials, respectively; ρ_c and ρ_m are the density of ceramic and metal materials, respectively; p is the volume fraction index of materials; v is the Poisson's ratios of ceramics and metals. Free vibration characteristics of functionally gradient beams based on first-order shear theory, the axial u and transverse displacements w at any point of a beam could be expressed as Eq. (2).

$$u(x,z,t) = u_0(x,t) - z\varphi(x,t), w(x,z,t) = w_0(x,t) \tag{2}$$

The geometric equation is Eq. (3).

$$\begin{cases} \varepsilon_x(x,z,t) = \dfrac{du_0}{dx} - z\dfrac{d\varphi}{dx} \\ \gamma_{xz}(x,z,t) = \dfrac{dw_0}{dx} - \varphi \end{cases} \tag{3}$$

where u_0 and w_0 are the axial and transverse displacement at any beam point, respectively; φ is the cross-section angle; ε_x and γ_{xz} are the linear strains and shear strains at any point on the cross-section, respectively. Based on the basic theory of Timoshenko beams, the normal stress σ_x and shear stress τ_{xz} on the cross-section could be expressed as Eq. (4).

$$\begin{cases} \sigma_x = E(z)\,\varepsilon_x = E(z)\left(\dfrac{du_0}{dx} - z\dfrac{d\varphi}{dx}\right) \\ \tau_{xz} = \dfrac{G(z)\,\gamma_{xz}}{\kappa} = \dfrac{E(z)}{2(1+\nu)\kappa}\left(\dfrac{dw_0}{dx} - \varphi\right) \end{cases} \tag{4}$$

where $E(z)$ and $G(z)$ are the elastic modulus and shear elastic modulus of the materials, respectively; ν is the Poisson's ratio, $\kappa = 6/5$ is the correction factor of a Timoshenko rectangular cross-section beam. Based on Eq. (4), the expressions of bending moment M, axial force F_N, and shear force Q in any section of the beam were stated as:

$$\begin{aligned} M &= \int_A \sigma_{xx} z dA = \int_A E(z)\, z\left(\frac{\partial u_0(x,t)}{\partial x} - z\frac{\partial \varphi(x,t)}{\partial x}\right) dA \\ &= \frac{\partial u_0(x,t)}{\partial x}\int_A E(z)\, z dA - \frac{\partial \varphi(x,t)}{\partial x}\int_A E(z)\, z^2 dA = D_1\frac{\partial u_0(x,t)}{\partial x} - D_2\frac{\partial \varphi(x,t)}{\partial x} \end{aligned} \tag{5a}$$

$$\begin{aligned} F_N &= \int_A \sigma_{xx} dA = \int_A E(z)\left(\frac{\partial u_0(x,t)}{\partial x} - z\frac{\partial \varphi(x,t)}{\partial x}\right) dA \\ &= \frac{\partial u_0(x,t)}{\partial x}\int_A E(z)\, dA - \frac{\partial \varphi(x,t)}{\partial x}\int_A E(z)\, z dA = D_0\frac{\partial u_0(x,t)}{\partial x} - D_1\frac{\partial \varphi(x,t)}{\partial x} \end{aligned} \tag{5b}$$

$$\begin{aligned} Q &= \int_A \tau_{xz} dA = \int_A \frac{G(z)\,\gamma_{xz}}{\kappa} dA = \int_A \frac{E(z)}{2(1+\nu)\kappa}\left(\frac{\partial w_0(x,t)}{\partial x} - \varphi(x,t)\right) dA \\ &= \left(\frac{\partial w_0(x,t)}{\partial x} - \varphi(x,t)\right)\int_A \frac{E(z)}{2(1+\nu)\kappa} dA = D_{xz}\left(\frac{\partial w_0(x,t)}{\partial x} - \varphi(x,t)\right) \end{aligned} \tag{5c}$$

where

$$D_0 = \int_A E(z)\, dA = \int_A E_m\left[1 + \left(\frac{E_c}{E_m} - 1\right)\left(\frac{1}{2} - \frac{z}{h}\right)^p\right] dA = E_m bh\left(1 + \frac{E_r - 1}{p+1}\right) = E_m bh\phi_0 \tag{6a}$$

$$D_1 = \int_A E(z)\, z dA = \int_A E_m\left[1 + \left(\frac{E_c}{E_m} - 1\right)\left(\frac{1}{2} - \frac{z}{h}\right)^p\right] z dA = E_m bh^2\frac{-(E_r - 1)\,p}{2(p+1)(p+2)} = E_m bh^2\phi_1 \tag{6b}$$

$$D_2 = \int_A E(z) z^2 dA = \int_A E_m \left[1 + \left(\frac{E_c}{E_m} - 1\right)\left(\frac{1}{2} - \frac{z}{h}\right)^p\right] z^2 dA = \frac{E_m b h^3}{12}\left[1 + \frac{3(E_r - 1)(p^2 + p + 2)}{(p+1)(p+2)(p+3)}\right]$$
$$= \frac{E_m b h^3}{12}\phi_2 \tag{6c}$$

where

$$E_r = \frac{E_c}{E_m}, \phi_0 = 1 + \frac{E_r - 1}{p+1}, \phi_1 = (E_r - 1)\frac{-p}{2(p+1)(p+2)}, \phi_2 = 1 + \frac{3(E_r - 1)(p^2 + p + 2)}{(p+1)(p+2)(p+3)}$$

As the beam was bent within the plane of its longitudinal symmetry, the equilibrium equations in the x and z directions were considered as follows:

$$\begin{cases} \dfrac{\partial \sigma_x}{\partial x} + \dfrac{\partial \tau_{xz}}{\partial z} = \rho(z)\dfrac{\partial^2 u}{\partial t^2} \\ \dfrac{\partial \sigma_z}{\partial z} + \dfrac{\partial \tau_{xz}}{\partial x} = \rho(z)\dfrac{\partial^2 w}{\partial t^2} \end{cases} \tag{7}$$

Then, Eq. (7) is integrated to derive Eq. (8).

$$\begin{cases} \int_A \left(\dfrac{\partial \sigma_x}{\partial x} + \dfrac{\partial \tau_{xz}}{\partial z}\right) dA = \int_A \rho(z)\dfrac{\partial^2 u}{\partial t^2} dA \\ \int_A \left(\dfrac{\partial \sigma_x}{\partial x} + \dfrac{\partial \tau_{xz}}{\partial z}\right) z dA = \int_A z\rho(z)\dfrac{\partial^2 u}{\partial t^2} dA \\ \int_A \left(\dfrac{\partial \sigma_z}{\partial z} + \dfrac{\partial \tau_{xz}}{\partial x}\right) dA = \int_A \rho(z)\dfrac{\partial^2 w}{\partial t^2} dA \end{cases} \tag{8}$$

Substituting Eq. (2) into Eq. (8) yields the following:

$$\begin{cases} \int_A \left(\dfrac{\partial \sigma_x}{\partial x} + \dfrac{\partial \tau_{xz}}{\partial z}\right) dA = \int_A \rho(z)\left(\dfrac{\partial^2 u_0}{\partial t^2} - z\dfrac{\partial^2 \varphi}{\partial t^2}\right) dA = I_0\dfrac{\partial^2 u_0}{\partial t^2} - I_1\dfrac{\partial^2 \varphi}{\partial t^2} \\ \int_A \left(\dfrac{\partial \sigma_x}{\partial x} + \dfrac{\partial \tau_{xz}}{\partial z}\right) z dA = \int_A z\rho(z)\left(\dfrac{\partial^2 u_0}{\partial t^2} - z\dfrac{\partial^2 \varphi}{\partial t^2}\right) dA = I_1\dfrac{\partial^2 u_0}{\partial t^2} - I_2\dfrac{\partial^2 \varphi}{\partial t^2} \\ \int_A \left(\dfrac{\partial \sigma_z}{\partial z} + \dfrac{\partial \tau_{xz}}{\partial x}\right) dA = \int_A \rho(z)\dfrac{\partial^2 w_0}{\partial t^2} dA = I_0\dfrac{\partial^2 w_0}{\partial t^2} \end{cases} \tag{9}$$

where

$$I_0 = \int_A \rho(z) dA = \int_A \rho_m \left[1 + \left(\frac{\rho_c}{\rho_m} - 1\right)\left(\frac{1}{2} - \frac{z}{h}\right)^p\right] dA = \rho_m b h\left(1 + \frac{\rho_r - 1}{p+1}\right) = \rho_m b h\overline{\phi}_0 \tag{10a}$$

$$I_1 = \int_A \rho(z) z dA = \int_A \rho_m \left[1 + \left(\frac{\rho_c}{\rho_m} - 1\right)\left(\frac{1}{2} - \frac{z}{h}\right)^p\right] z dA = \rho_m b h^2 \frac{-(\rho_r - 1)p}{2(p+1)(p+2)} = \rho_m b h^2 \overline{\phi}_1 \tag{10b}$$

$$I_2 = \int_A \rho(z) z^2 dA = \int_A \rho_m \left[1 + \left(\frac{\rho_c}{\rho_m} - 1\right)\left(\frac{1}{2} - \frac{z}{h}\right)^p\right] z^2 dA = \frac{\rho_m b h^3}{12}\left[1 + \frac{3(\rho_r - 1)(p^2 + p + 2)}{(p+1)(p+2)(p+3)}\right]$$
$$= \frac{\rho_m b h^3}{12}\overline{\phi}_2 \tag{10c}$$

where

$$\rho_r = \frac{\rho_c}{\rho_m},\ \overline{\phi}_0 = 1 + \frac{\rho_r - 1}{p+1},\ \overline{\phi}_1 = \frac{-(\rho_r - 1)\,p}{2(p+1)(p+2)},\ \overline{\phi}_2 = 1 + \frac{3(\rho_r - 1)\left(p^2 + p + 2\right)}{(p+1)(p+2)(p+3)}$$

Further derivation of Eq. (9) gave

$$\frac{\partial F_N}{\partial x} = I_0 \frac{\partial^2 u_0}{\partial t^2} - I_1 \frac{\partial^2 \varphi}{\partial t^2} \tag{11a}$$

$$\frac{\partial M}{\partial x} - Q = I_1 \frac{\partial^2 u_0}{\partial t^2} - I_2 \frac{\partial^2 \varphi}{\partial t^2} \tag{11b}$$

$$\frac{\partial Q}{\partial x} - q = I_0 \frac{\partial^2 w_0}{\partial t^2} \tag{11c}$$

Substituting Eq. (5) into Eq. (11), the equilibrium differential equation for free vibration is derived, considering the shear deformation and rotational inertia of the beam section.

$$\begin{cases} D_0 \dfrac{\partial^2 u_0(x,t)}{\partial x^2} - D_1 \dfrac{\partial^2 \varphi(x,t)}{\partial x^2} = I_0 \dfrac{\partial^2 u_0}{\partial t^2} - I_1 \dfrac{\partial^2 \varphi}{\partial t^2} \\ D_1 \dfrac{\partial^2 u_0(x,t)}{\partial x^2} - D_2 \dfrac{\partial^2 \varphi(x,t)}{\partial x^2} - D_{xz}\left(\dfrac{\partial w_0(x,t)}{\partial x} - \varphi(x,t)\right) = I_1 \dfrac{\partial^2 u_0}{\partial t^2} - I_2 \dfrac{\partial^2 \varphi}{\partial t^2} \\ D_{xz}\left(\dfrac{\partial^2 w_0(x,t)}{\partial x^2} - \dfrac{\partial \varphi(x,t)}{\partial x}\right) = q + I_0 \dfrac{\partial^2 w_0}{\partial t^2} \end{cases} \tag{12}$$

Considering the free vibration of a beam, then the axial displacement u_0, transverse displacement w_0, and cross-section angle φ can be expressed as Eq. (13).

$$\left(u_0(x,t), w_0(x,t), \varphi(x,t)\right) = \left(\widehat{u}(x), \widehat{w}(x), \widehat{\varphi}(x)\right)\cos\omega t \tag{13}$$

where ω is the circular frequency of a beam, $\widehat{u}(x), \widehat{w}(x), \widehat{\varphi}(x)$ are the vibration modal functions. Substitute Eqs. (1), (2), (4), and (13) into Eq. (12). Dimensionless transformation $\left(\xi, \widehat{U}, \widehat{W}\right) = \left(x, \widehat{u}, \widehat{w}\right)/L$, the equilibrium differential equation of a Timoshenko beam with FGMs was obtained as Eq. (14).

$$\begin{cases} \widehat{U}''(\xi) - a_1 \widehat{W}'(\xi) + a_1 \widehat{\varphi}(\xi) - a_2 \lambda \widehat{U}(\xi) - a_3 \lambda \widehat{\varphi}(\xi) = 0 \\ \widehat{\varphi}''(\xi) + a_4 \widehat{W}'(\xi) - a_4 \widehat{\varphi}(\xi) - a_5 \lambda \widehat{U}(\xi) - a_6 \lambda \widehat{\varphi}(\xi) = 0 \\ \widehat{W}''(\xi) - \widehat{\varphi}'(\xi) + \alpha_7 \lambda \widehat{W}(\xi) = 0 \end{cases} \tag{14}$$

where

$$a_1 = \frac{6c\phi_2}{\kappa\delta(1+\nu)}, a_2 = \delta^2\left[\frac{c\phi_2}{\phi_1}\left(\overline{\phi}_2 - \frac{\phi_2\overline{\phi}_1}{\phi_1}\right) - \frac{\overline{\phi}_1}{12\phi_1}\right], a_3 = \delta^3\left[\frac{c\phi_2}{\phi_1}\left(\frac{\phi_2\overline{\phi}_2}{\phi_1} - \frac{\overline{\phi}_3}{12}\right) + \frac{\overline{\phi}}{12\phi_1}\right]$$

$$a_4 = \frac{6c\phi_1}{\kappa\delta^2(1+\nu)}, a_5 = c\delta\left(\overline{\phi}_2 - \frac{\phi_2\overline{\phi}_1}{\phi_1}\right), a_6 = c\delta^2\left(\frac{\phi_2\overline{\phi}_2}{\phi_1} - \frac{\overline{\phi}_3}{12}\right), a_7 = \frac{\kappa(1+\nu)\overline{\phi}_1\delta^2}{6\phi_1}$$

where $c = \frac{1}{\phi_3 - 12\phi_2^2/\phi_1}$ is the coefficient related to the gradient change law of material properties; $\delta = h/L$ is the height-span ratio of a rectangular cross-section beam; $\lambda = \frac{\rho_m A L^4 \omega^2}{E_m I}$ is the dimensionless frequency

of a beam. The six dimensionless coefficients were as follows:

$$\phi_1 = 1 + \frac{\alpha}{p+1}, \phi_2 = -\frac{\alpha p}{2(p+1)(p+2)}, \phi_3 = 1 + \frac{3\alpha(p^2+p+2)}{(p+1)(p+2)(p+3)}$$

$$\overline{\phi}_1 = 1 + \frac{\beta}{p+1}, \overline{\phi}_2 = -\frac{\beta p}{2(p+1)(p+2)}, \overline{\phi}_3 = 1 + \frac{3\beta(p^2+p+2)}{(p+1)(p+2)(p+3)}$$

where $K = E_c/E_m$, $\alpha = K - 1$, $\overline{K} = \rho_c/\rho_m$, $\beta = \overline{K} - 1$.

The boundary condition of simply supported (S-S) beams:

$$\widehat{U}(0) = 0, \widehat{W}(0) = 0, \widehat{\varphi}'(0) = 0 \tag{15a}$$

$$\widehat{U}(1) = 0, \widehat{W}(1) = 0, \widehat{\varphi}'(1) = 0 \tag{15b}$$

The boundary condition of clamped-clamped (C-C) beams:

$$\widehat{U}(0) = 0, \widehat{W}(0) = 0, \widehat{\varphi}(0) = 0 \tag{15c}$$

$$\widehat{U}(1) = 0, \widehat{W}(1) = 0, \widehat{\varphi}(1) = 0 \tag{15d}$$

The boundary condition of free-free (F-F) beams:

$$\widehat{U}'(0) = 0, \widehat{W}'(0) - \widehat{\varphi}(0) = 0, \widehat{\varphi}'(0) = 0 \tag{15e}$$

$$\widehat{U}'(1) = 0, \widehat{W}'(1) - \widehat{\varphi}(1) = 0, \widehat{\varphi}'(1) = 0 \tag{15f}$$

The boundary condition of clamped-free (C-F) beams:

$$\widehat{U}(0) = 0, \widehat{W}(0) = 0, \widehat{\varphi}(0) = 0 \tag{15g}$$

$$\widehat{U}'(1) = 0, \widehat{W}'(1) - \widehat{\varphi}(1) = 0, \widehat{\varphi}'(1) = 0 \tag{15h}$$

2.2 Beam Theory of Ignoring the Shear Deformation of the Beam Section and Only Considering the Effect of the Rotational Inertia of the Cross-Section

If the shear deformation was neglected and only the case of rotational inertia of the beam section was considered, the axial displacement u_0, transverse displacement w_0, and section turning angle φ needed to be decoupled in the derivation of the equation. Firstly, the $\frac{\partial u_0(x,t)}{\partial x}$ is solved from Eq. (5b),

$$\frac{\partial u_0(x,t)}{\partial x} = \frac{1}{D_0}\left[F_N + D_1\frac{\partial \varphi(x,t)}{\partial x}\right] \tag{16}$$

Substituting Eq. (16) into Eq. (5a), it is obtained

$$M = \left(\frac{D_1^2}{D_0} - D_2\right)\frac{\partial \varphi(x,t)}{\partial x} + \frac{D_1}{D_0}F_N \tag{17}$$

Similarly, according to Eq. (11a)

$$\frac{\partial^2 u_0}{\partial t^2} = \frac{1}{I_0}\frac{\partial F_N}{\partial x} + \frac{I_1}{I_0}\frac{\partial^2 \varphi}{\partial t^2} = \frac{I_1}{I_0}\frac{\partial^2 \varphi}{\partial t^2} \tag{18}$$

By substituting Eq. (18) into Eq. (11b), it is obtained

$$\frac{\partial M}{\partial x} - Q = \frac{I_1}{I_0}\frac{\partial F_N}{\partial x} + \left(\frac{I_1^2}{I_0} - I_2\right)\frac{\partial^2 \varphi}{\partial t^2} \tag{19}$$

Suppose $q = 0$. In this study, the pure bending deformation of a beam was investigated, as well as the symmetric distribution of the material properties, so that $F_N = 0$, associating Eqs. (11c) and (19), it was obtained

$$\frac{\partial Q}{\partial x} = I_0\frac{\partial^2 w_0}{\partial t^2} \tag{20a}$$

$$\frac{\partial M}{\partial x} - Q = \left(\frac{I_1^2}{I_0} - I_2\right)\frac{\partial^2 \varphi}{\partial t^2} \tag{20b}$$

Substituting Eqs. (17) and (5c) into Eqs. (20), the derivative was simplified to obtain

$$\frac{\partial^2}{\partial x^2}\left[\left(\frac{D_1^2}{D_0} - D_2\right)\frac{\partial \varphi}{\partial x}\right] - I_0\frac{\partial^2 w_0}{\partial t^2} - \left(\frac{I_1^2}{I_0} - I_2\right)\frac{\partial^3 \varphi}{\partial x \partial t^2} = 0 \tag{21}$$

If the shear deformation is not considered, it can be obtained by substituting $\gamma_{xz} = 0$, $\varphi = \dfrac{\partial w_0}{\partial x}$ into Eq. (21).

$$\frac{\partial^2}{\partial x^2}\left[\left(\frac{D_1^2}{D_0} - D_2\right)\frac{\partial^2 w_0}{\partial x^2}\right] - I_0\frac{\partial^2 w_0}{\partial t^2} - \left(\frac{I_1^2}{I_0} - I_2\right)\frac{\partial^4 w_0}{\partial x^2 \partial t^2} = 0 \tag{22}$$

Supposing $\xi = x/L$, $w_0(x,t) = \widehat{w}(x)\cos\omega t$, then Eq. (22) is transformed into

$$\left(\frac{D_1^2}{D_0} - D_2\right)\frac{d^4\widehat{w}(\xi)}{d\xi^4} + \omega^2 I_0 L^4 \widehat{w}(\xi) + \omega^2 L^2\left(\frac{I_1^2}{I_0} - I_2\right)\frac{d^2\widehat{w}(\xi)}{d\xi^2} = 0 \tag{23}$$

Substituting Eqs. (6) and (10) into Eq. (23) and $\Omega^2 = \frac{\omega^2 \rho_m A L^4}{E_m I}$, it is obtained

$$\frac{d^4\widehat{w}(\xi)}{d\xi^4} + \Omega^2\frac{\overline{\phi}_0\phi_0}{12\phi_1^2 - \phi_0\phi_2}\widehat{w}(\xi) + \Omega^2\frac{\delta^2\phi_0\left(12\overline{\phi}_1^2 - \overline{\phi}_0\overline{\phi}_2\right)}{12\overline{\phi}_0\left(12\phi_1^2 - \phi_0\phi_2\right)}\frac{d^2\widehat{w}(\xi)}{d\xi^2} = 0 \tag{24}$$

Thus, the natural frequency calculation of the functional gradient beam was transformed into the problem of solving Eqs. (16) and (24) under boundary conditions Eq. (10).

2.3 Theory of Improved DQM

This study applies the improved differential quadrature method to calculate the free vibration natural frequencies of functionally graded beams. The accuracy of the differential quadrature method depends on the discrete node step size and the weight coefficient matrix A(r), which is influenced by the distribution of nodes and the number of nodes. The normalized beam length interval [0,1] was divided into N discrete elements, resulting in a total of N+1, discrete nodes, denoted by $\xi_j (0 \le j \le N)$, assuming $\xi_0 = 0, \xi_N = 1$. The sudden change in the beam's stiffness near the ends of the supports, or the influence of the end boundary conditions, made the vicinity of the beam's end the most sensitive region for displacement and internal force changes. Therefore, arranging more fine-grained, non-uniform nodes in the two end regions of the beam improved the calculation accuracy. This study adopts a distribution of discrete nodes in a discrete form of geometric sequence nodes as described in Eq. (25), i.e.,

$$\begin{cases} \xi_i = a + \dfrac{b-a}{2\left(q_1^{n/2}-1\right)}\left(q_1^i - 1\right), \left(\mathrm{q}_1 \geq 1.0, i = 0, 1, 2, \cdots, \dfrac{n}{2}\right) \\ \xi_i = b - \dfrac{b-a}{2\left(q_2^{n/2}-1\right)}\left(q_2^{n-i} - 1\right), \left(\mathrm{q}_2 = \dfrac{1}{q_1}, i = \dfrac{n}{2}, \dfrac{n}{2}+1, \ldots, n\right) \end{cases} \tag{25}$$

The nodes are distributed from the end of the beam to the center in a series of equal ratios with the common ratio q, which can control the numerical calculation accuracy and numerical dissipation by adjusting the common ratio to modify the step size of the nodes for a certain number of discrete n.

The function $\widehat{U}(\xi)$, $\widehat{W}(\xi)$ and $\widehat{\varphi}(\xi)$ are described using the Lagrange interpolation function as Eq. (26).

$$\begin{cases} \widehat{U}(\xi) = \sum_{j=0}^{N} l_j(\xi)\,\widehat{U}\left(\xi_j\right) \\ \widehat{W}(\xi) = \sum_{j=0}^{N} l_j(\xi)\,\widehat{W}\left(\xi_j\right) \\ \widehat{\varphi}(\xi) = \sum_{j=0}^{N} l_j(\xi)\,\widehat{\varphi}\left(\xi_j\right) \end{cases} \tag{26}$$

where $l_j(\xi)$ is Lagrange polynomial, and it is stated as Eq. (27).

$$l_j(\xi) = \prod_{\substack{k=0 \\ k \neq j}}^{N} \frac{\xi - \xi_k}{\xi_j - \xi_k} \tag{27}$$

From Eq. (26), the first derivative of the function $\widehat{U}(\xi)$, $\widehat{W}(\xi)$ and $\widehat{\varphi}(\xi)$ is obtained, the function and its derivatives at each node were represented by a weighted linear sum of the values of discrete $N+1$ node functions.

$$\begin{cases} \widehat{U}'(\xi_i) = \sum_{j=0}^{N} l_j'(\xi_i)\,\widehat{U}\left(\xi_j\right) \\ \widehat{W}'(\xi_i) = \sum_{j=0}^{N} l_j'(\xi_i)\,\widehat{W}\left(\xi_j\right) \\ \widehat{\varphi}'(\xi_i) = \sum_{j=0}^{N} l_j'(\xi)\,\widehat{\varphi}\left(\xi_j\right) \end{cases} \tag{28}$$

Eq. (28) is rewritten in vector form as follows:

$$\begin{cases} \widehat{\boldsymbol{U}}' = \boldsymbol{A}_{ij}^{(1)}\widehat{\boldsymbol{U}} \\ \widehat{\boldsymbol{W}}' = \boldsymbol{A}_{ij}^{(1)}\widehat{\boldsymbol{W}} \\ \widehat{\boldsymbol{\varphi}}' = \boldsymbol{A}_{ij}^{(1)}\widehat{\boldsymbol{\varphi}} \end{cases} \tag{29}$$

where the weight coefficient matrix $\boldsymbol{A}_{ij}^{(1)}$ is expressed as follows:

$$\boldsymbol{A}_{ij}^{(1)} = \left(A_{ij}^{(1)}\right)_{(N+1)\times(N+1)} \tag{30}$$

where $A_{ij}^{(1)}$ is expressed as Eq. (31).

$$A_{ij}^{(1)} = l_j'(\xi_i) = \begin{cases} \prod\limits_{\substack{k=0 \\ k \neq i,j}}^{N} (\xi_i - \xi_k) \Big/ \prod\limits_{\substack{k=0 \\ k \neq i,j}}^{N} (\xi_j - \xi_k) \ (i \neq j) \\ \sum\limits_{\substack{k=0 \\ k \neq i}}^{N} \dfrac{1}{(\xi_i - \xi_k)} \ (i = j) \end{cases} \tag{31}$$

In Eq. (29), the column vectors $\widehat{\boldsymbol{U}}'$, $\widehat{\boldsymbol{U}}$, $\widehat{\boldsymbol{W}}'$, $\widehat{\boldsymbol{W}}$, $\widehat{\boldsymbol{\varphi}}'$ and $\widehat{\boldsymbol{\varphi}}$ are as follows:

$$\begin{cases} \widehat{\boldsymbol{U}}' = \left(\widehat{U}'(\xi_0), \quad \widehat{U}'(\xi_1), \quad \cdots, \quad \widehat{U}'(\xi_N)\right)^{\mathrm{T}}, \widehat{\boldsymbol{U}} = \left(\widehat{U}(\xi_0), \quad \widehat{U}(\xi_1), \quad \cdots, \quad \widehat{U}(\xi_N)\right)^{\mathrm{T}} \\ \widehat{\boldsymbol{W}}' = \left(\widehat{W}'(\xi_0), \quad \widehat{W}'(\xi_1), \quad \cdots, \quad \widehat{W}'(\xi_N)\right)^{\mathrm{T}}, \widehat{\boldsymbol{W}} = \left(\widehat{W}(\xi_0), \quad \widehat{W}(\xi_1), \quad \cdots, \quad \widehat{W}(\xi_N)\right)^{\mathrm{T}} \\ \widehat{\boldsymbol{\varphi}}' = \left(\widehat{\varphi}'(\xi_0), \quad \widehat{\varphi}'(\xi_1), \quad \cdots, \quad \widehat{\varphi}'(\xi_N)\right)^{\mathrm{T}}, \widehat{\boldsymbol{\varphi}} = \left(\widehat{\varphi}(\xi_0), \quad \widehat{\varphi}(\xi_1), \quad \cdots, \quad \widehat{\varphi}(\xi_N)\right)^{\mathrm{T}} \end{cases} \tag{32}$$

Similarly, from Eq. (29), it can be inferred that Eq. (33).

$$\begin{cases} \widehat{\boldsymbol{U}}'' = \boldsymbol{A}_{ij}^{(2)} \widehat{\boldsymbol{U}} \\ \widehat{\boldsymbol{W}}'' = \boldsymbol{A}_{ij}^{(2)} \widehat{\boldsymbol{W}} \\ \widehat{\boldsymbol{\varphi}}'' = \boldsymbol{A}_{ij}^{(2)} \widehat{\boldsymbol{\varphi}} \end{cases} \tag{33}$$

The column vectors $\widehat{\boldsymbol{U}}''$, $\widehat{\boldsymbol{W}}''$ and $\widehat{\boldsymbol{\varphi}}''$ are as follows:

$$\begin{cases} \widehat{\boldsymbol{U}}'' = \left(\widehat{U}''(\xi_0), \quad \widehat{U}''(\xi_1), \quad \cdots, \quad \widehat{U}''(\xi_N)\right)^{\mathrm{T}} \\ \widehat{\boldsymbol{W}}'' = \left(\widehat{W}''(\xi_0), \quad \widehat{W}''(\xi_1), \quad \cdots, \quad \widehat{W}''(\xi_N)\right)^{\mathrm{T}} \\ \widehat{\boldsymbol{\varphi}}'' = \left(\widehat{\varphi}''(\xi_0), \quad \widehat{\varphi}''(\xi_1), \quad \cdots, \quad \widehat{\varphi}''(\xi_N)\right)^{\mathrm{T}} \end{cases} \tag{34}$$

where the relationship between weight coefficient matrices $\boldsymbol{A}_{ij}^{(2)}$ and $\boldsymbol{A}_{ij}^{(1)}$ is Eq. (35).

$$\boldsymbol{A}_{ij}^{(2)} = \boldsymbol{A}_{ij}^{(1)} \boldsymbol{A}_{ij}^{(1)} \tag{35}$$

The boundary conditions of beams were discussed by taking C-C beams as an example. Substituting Eqs. (29) and (33) into Eqs. (15c) and (15d), it can be obtained Eq. (36).

$$[\boldsymbol{I}]_{I_l=0} \widehat{\boldsymbol{U}} = \boldsymbol{0}, [\boldsymbol{I}]_{I_l=0} \widehat{\boldsymbol{W}} = \boldsymbol{0}, [\boldsymbol{I}]_{I_l=0} \widehat{\boldsymbol{\varphi}} = \boldsymbol{0} \tag{36a}$$

$$[\boldsymbol{I}]_{I_l=1} \widehat{\boldsymbol{U}} = \boldsymbol{0}, [\boldsymbol{I}]_{I_l=1} \widehat{\boldsymbol{W}} = \boldsymbol{0}, [\boldsymbol{I}]_{I_l=1} \widehat{\boldsymbol{\varphi}} = \boldsymbol{0} \tag{36b}$$

where I_l is the elements of I_l-th row with 0 and n, $[\cdots]_{I_l}$ is a matrix, $\boldsymbol{I}$ is the identity matrix of order $(n+1) \times (n+1)$. Substituting Eqs. (29) and (33) into Eq. (16), the equation of motion of a FGMs beam is obtained as Eq.(37).

$$\begin{bmatrix} \boldsymbol{A}_{ij}^{(2)} & -a_1 \boldsymbol{A}_{ij}^{(1)} & a_1 \boldsymbol{I} \\ \boldsymbol{0} & a_4 \boldsymbol{A}_{ij}^{(1)} & \boldsymbol{A}_{ij}^{(2)} - a_4 \boldsymbol{I} \\ \boldsymbol{0} & \boldsymbol{A}_{ij}^{(2)} & -\boldsymbol{A}_{ij}^{(1)} \end{bmatrix} \begin{pmatrix} \widehat{\boldsymbol{U}} \\ \widehat{\boldsymbol{W}} \\ \widehat{\boldsymbol{\varphi}} \end{pmatrix} - \lambda \begin{bmatrix} a_2 \boldsymbol{I} & \boldsymbol{0} & a_3 \boldsymbol{I} \\ a_5 \boldsymbol{I} & \boldsymbol{0} & a_6 \boldsymbol{I} \\ \boldsymbol{0} & -\alpha_7 \boldsymbol{I} & \boldsymbol{0} \end{bmatrix} \begin{pmatrix} \widehat{\boldsymbol{U}} \\ \widehat{\boldsymbol{W}} \\ \widehat{\boldsymbol{\varphi}} \end{pmatrix} = \begin{pmatrix} \boldsymbol{0} \\ \boldsymbol{0} \\ \boldsymbol{0} \end{pmatrix} \tag{37}$$

Simultaneous Eqs. (36) and (37) that was the I_l-th row constant coefficient followed by replacing the first row and last row of the corresponding matrix of Eq. (37). Thus, based on the above formula, a general program was written in FORTRAN language to solve the natural frequency of the FGMs beams along the thickness direction.

3 Numerical Examples and Discussion

3.1 DQM

Functionally graded materials are composed of metal material aluminum and ceramic material Al_2O_3, the material parameters of the FGMs in Eq. (1) are listed in Table 1.

Table 1: Two physical parameters of functionally graded materials

Type	Elasticity modulus	Density	Poisson's ratio
AL_2O_3	380 GPa	3800 kg/m^3	0.23
AL	70 GPa	2700 kg/m^3	0.23

Take the number of discrete units of beam length as N = 20, solving Eq. (24) by DQM. Tables 2–5 show the dimensionless natural frequency Ω_1 of FGMs beams with different boundary conditions, and material gradient parameter p are calculated by DQM.

Table 2: Dimensionless natural frequencies Ω_1 of FGMs beams with S-S boundary conditions

BC	δ	p							
		0	1	3	5	7	10	100	∞
S-S	0.2	30.4461	16.7006	13.4529	12.6765	12.2492	11.8228	10.0676	9.71116
	0.1	30.8164	16.8880	13.5973	12.8140	12.3839	11.9551	10.1885	9.82927
	0.05	30.9111	16.9359	13.6342	12.8490	12.4183	11.9888	10.2194	9.85948
	0.02	30.9377	16.9494	13.6445	12.8589	12.4279	11.9983	10.2281	9.86799
	0.01	30.9416	16.9513	13.6460	12.8603	12.4293	11.9997	10.2294	9.86920
	0.005	30.9425	16.9518	13.6464	12.8607	12.4297	12.0000	10.2297	9.86951
	0.002	30.9428	16.9519	13.6465	12.8608	12.4298	12.0001	10.2298	9.86959
	Ref. [23]	30.944	16.952	13.647	12.861	12.430	12.000	10.230	9.8696

Table 3: Dimensionless natural frequencies Ω_1 of FGMs beams with C-S boundary conditions

BC	δ	p							
		0	1	3	5	7	10	100	∞
C-S	0.2	47.4365	26.0256	20.9668	19.7563	19.0897	18.4243	15.6863	15.1304
	0.1	48.1084	26.3659	21.2289	20.0058	19.3342	18.6645	15.9058	15.3448
	0.05	48.2808	26.4530	21.2960	20.0697	19.3968	18.7260	15.9621	15.3997
	0.02	48.3294	26.4776	21.3149	20.0876	19.4144	18.7433	15.9779	15.4152
	0.01	48.3364	26.4811	21.3176	20.0902	19.4169	18.7458	15.9802	15.4175
	0.005	48.3381	26.4819	21.3183	20.0909	19.4175	18.7464	15.9808	15.4180
	0.002	48.3386	26.4822	21.3185	20.0910	19.4177	18.7466	15.9809	15.4182
	Ref. [23]	48.341	26.483	21.319	20.091	19.418	18.747	15.981	15.418

Table 4: Dimensionless natural frequencies Ω_1 of FGMs beams with C-C boundary conditions

BC	δ	p							
		0	1	3	5	7	10	100	∞
C-C	0.2	68.7474	37.7213	30.3907	28.6358	27.6691	26.7042	22.7337	21.9278
	0.1	69.7874	38.2480	30.7965	29.0220	28.0476	27.0759	23.0734	22.2595
	0.05	70.0545	38.3831	30.9004	29.1210	28.1446	27.1712	23.1607	22.3447
	0.02	70.1299	38.4211	30.9297	29.1488	28.1719	27.1981	23.1853	22.3688
	0.01	70.1407	38.4266	30.9339	29.1528	28.1758	27.2019	23.1888	22.3722
	0.005	70.1434	38.4279	30.9349	29.1538	28.1768	27.2029	23.1897	22.3731
	0.002	70.1441	38.4283	30.9352	29.1541	28.1771	27.2031	23.1899	22.3733
	Ref. [23]	70.147	38.429	30.935	29.154	28.177	27.203	23.189	22.373

Table 5: Dimensionless natural frequencies Ω_1 of FGMs beams with C-F boundary conditions

BC	δ	p							
		0	1	3	5	7	10	100	∞
C-F	0.2	11.0391	6.04708	4.86768	4.58748	4.43382	4.28067	3.64951	3.52106
	0.1	11.0272	6.04108	4.86306	4.58309	4.42951	4.27643	3.64563	3.51727
	0.05	11.0242	6.03958	4.86191	4.58199	4.42844	4.27538	3.64467	3.51633
	0.02	11.0234	6.03916	4.86159	4.58168	4.42814	4.27508	3.64440	3.51606
	0.01	11.0233	6.03910	4.86154	4.58164	4.42810	4.27504	3.64436	3.51602
	0.005	11.0233	6.03909	4.86153	4.58163	4.42809	4.27503	3.64435	3.51601
	0.002	11.0232	6.03909	4.86153	4.58163	4.42808	4.27503	3.64434	3.51601
	Ref. [23]	11.024	6.0392	4.8616	4.5816	4.4281	4.2750	3.6443	3.5160

Tables 2–5 demonstrate that the results are consistent with the solution presented in reference [23], showing that as the height-span ratio h/L decreases, the section inertia of the beam has minimal impact on the natural frequency of slender beams. However, this effect is not negligible for short, thick beams.

To verify the feasibility and accuracy of calculating the natural frequencies of FGMs beams using DQM, assume $p = 0$, thereby simplifying an FGMs beam into a uniform ceramic beam. Tables 6–8 display the first ten natural frequencies for C-C, S-S, and C-F beams when the height-span ratio is $h/L = 0.002$ (with the number of discrete elements of the beam N = 20). As seen from Tables 6–8, numerical results show excellent consistency with those reported in references [2,3] and exact solutions, indicating that DQM is accurate for calculating the natural frequencies of beams made of isotropic homogeneous materials. Here, the natural frequencies of beams in Tables 6–8 and the dimensionless natural frequencies of beams in references [2,3] are defined as per Eq. (38).

$$\Omega = \sqrt[4]{\lambda \frac{\overline{\phi}_1}{\phi_3}} = \sqrt[4]{\frac{\omega^2 A L^4 \rho_m}{E_m I}} \sqrt[4]{\frac{\overline{\phi}_1}{\phi_3}} \tag{38}$$

Table 6: Normalized natural frequencies determined for C-C beam with $h/L = 0.002$ and $N = 20$

	$h/L = 0.002$			
Frequencies	Exact solution	Ref. [2]	Ref. [3]	Present method
Ω_1	4.73004	4.729979	4.72998	4.72997204
Ω_2	7.85320	7.852959	7.85296	7.85305051
Ω_3	10.9956	10.994991	10.9950	10.9956785
Ω_4	14.1372	14.135925	14.1360	14.1385691
Ω_5	17.2788	17.276580	17.2768	17.2840720
Ω_6	20.4204	20.416854	20.4174	20.4344743
Ω_7	23.5619	23.556687	23.5578	23.5931577
Ω_8	26.7035	26.696015	26.6980	26.7647568
Ω_9	29.8451	29.834775	29.8382	29.9553706
Ω_{10}	32.9867	32.972905	32.9786	33.1727843

Table 7: Normalized natural frequencies determined for S-S beam with $h/L = 0.002$ and $N = 20$

	$h/L = 0.002$			
Frequencies	Exact solution	Ref. [2]	Ref. [3]	Present method
Ω_1	3.14159	3.141327	3.14158	3.14158157
Ω_2	6.28319	6.281059	6.28310	6.28313451
Ω_3	9.42478	9.417609	9.42450	9.42481963
Ω_4	12.5664	12.549414	12.5657	12.5671771
Ω_5	15.7080	15.674921	15.7068	15.7113171
Ω_6	18.8496	18.792632	18.8476	18.8591123
Ω_7	21.9911	21.901049	21.9883	22.0133918
Ω_8	25.1327	24.998815	25.1288	25.1781397
Ω_9	28.2743	28.084502	28.2692	28.3586990
Ω_{10}	31.4159	31.156826	31.4098	31.5619876

Table 8: Normalized natural frequencies determined for C-F beam with $h/L = 0.002$ and $N = 20$

	$h/L = 0.002$			
Frequencies	Exact solution	Ref. [2]	Ref. [4]	Present method
Ω_1	1.8751	1.875103	1.87826	1.87510063
Ω_2	4.6936	4.694043	4.70199	4.69404075
Ω_3	7.8549	7.854556	7.86790	7.85466369
Ω_4	10.9955	10.995009	11.0138	10.9957282
Ω_5	14.1372	14.136069	14.1603	14.1387654
Ω_6	17.2788	17.276791	17.3066	17.2843612

(Continued)

Table 8 (continued)

Frequencies	$h/L = 0.002$			
	Exact solution	Ref. [2]	Ref. [4]	Present method
Ω_7	20.4204	20.417150	20.4525	20.4348796
Ω_8	23.5619	23.557080	23.5982	23.5936997
Ω_9	26.7035	26.696519	26.7434	26.7654578
Ω_{10}	29.8451	29.835404	29.8882	29.9562549

Assuming $p = 0$, Fig. 2 illustrates the curve of the first 15 natural frequencies of Timoshenko beams with varying height-to-span ratios h/L. As observed in Fig. 2: (a–d), for smaller values of h/L, i.e., $h/L = 0.002$ and 0.005, the relationship between non-dimensional frequency parameters and frequency orders is almost linear. This relationship becomes nonlinear with the increase in height-to-span ratios.

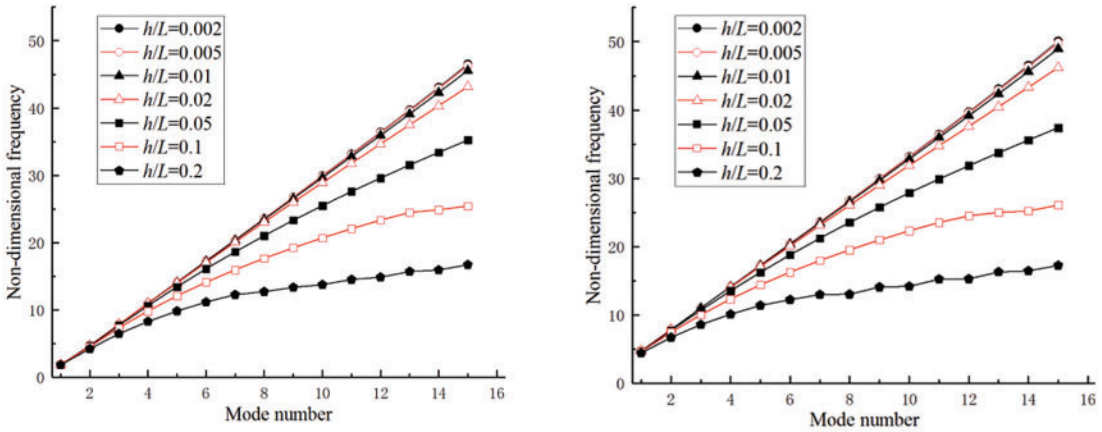

(a) C-F beam

(b) F-F beam

(c) C-C beam

(d) S-S beam

Figure 2: Non-dimensional frequency parameters Ω of the beam for different boundary conditions

Assuming $p = 0.3$, the first natural frequencies of FGMs beams were calculated using DQM. The results, listed in Table 9, show excellent consistency with those reported in references [24,25], proving that DQM is effective and accurate for calculating the natural frequencies of FGMs beams. The natural frequencies of beams in Table 9 and the dimensionless natural frequencies of beams in references [24,25] are defined as per Eq. (39).

$$\Omega = \sqrt{\lambda \frac{\overline{\phi}_1}{12\phi_1}} = \sqrt{\frac{\omega^2 AL^4 \rho_m}{E_m I}} \sqrt{\frac{\overline{\phi}_1}{12\phi_1}} \tag{39}$$

Table 9: First natural frequencies Ω_1 of FGMs beams with $p = 0.3$

Boundary condition	Method of calculation	h/L = 1/10	h/L = 1/30	h/L = 1/50	h/L = 1/100
S-S	Literature [24]	2.695	2.737	/	2.742
	Literature [25]	2.701	2.738	/	2.742
	DQM	2.702010	2.738123	2.741092	2.742348
C-F	Literature [24]	0.969	0.976	/	0.977
	Literature [25]	0.970	0.976	/	0.977
	DQM	0.9701438	0.9763097	0.9768091	0.9770201
C-C	Literature [24]	5.811	6.167	/	6.212
	Literature [25]	5.875	6.177	/	6.214
	DQM	5.869043	6.175456	6.202253	6.213671

Note: The "/" in Table 9 indicated that the calculated values were not given in the literature [24,25].

Based on first-order shear deformation theory, the governing Eq. (37) of a FGMs Timoshenko beam was calculated by DQM. The first natural frequency curve of the beam under different boundary conditions with material parameter p was obtained as shown in Figs. 3–5 ($0.0001 \leq p \leq 10000$).

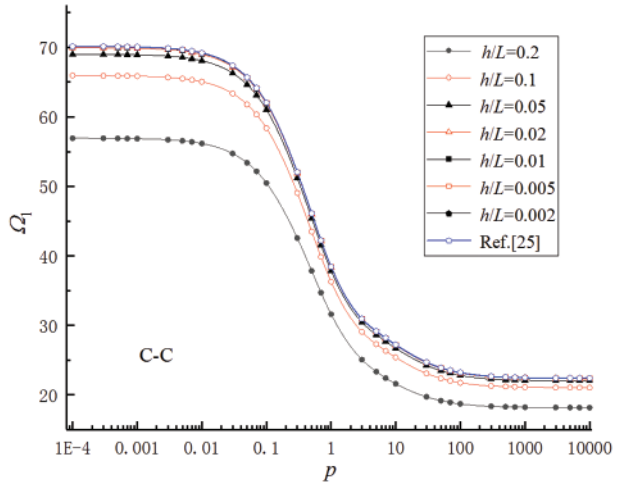

Figure 3: Relationships between the first natural frequencies Ω_1 and material parameter p for FGMs beams with boundary condition C-C

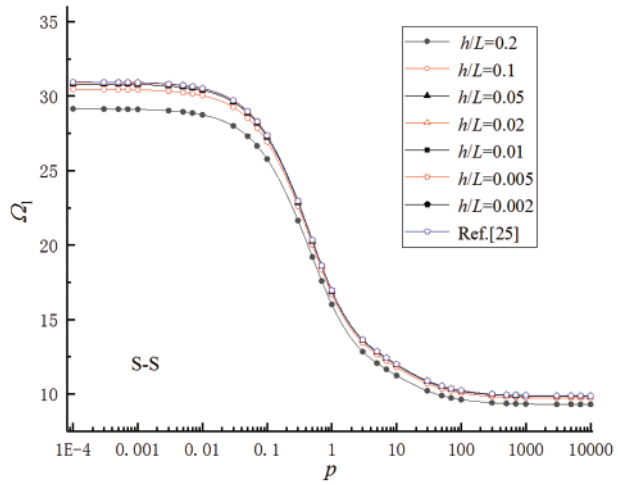

Figure 4: Relationships between the first natural frequencies Ω_1 and material parameter p for FGMs beams with boundary condition S-S

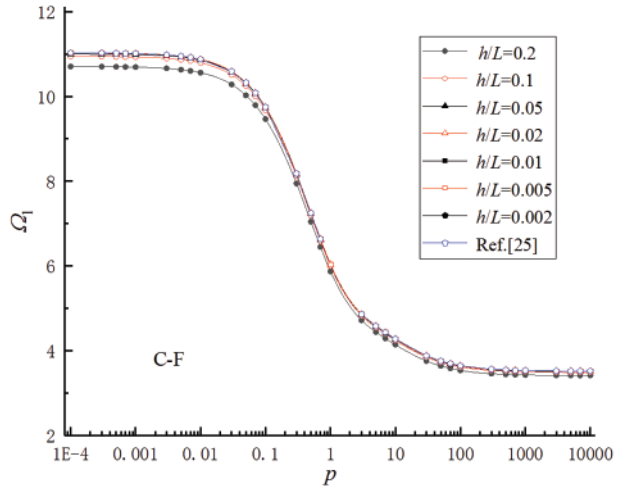

Figure 5: Relationships between the first natural frequencies Ω_1 and material parameter p for FGMs beams with boundary condition C-F

The variation in the gradient parameter primarily corresponds to alterations in physical properties such as material stiffness and density, which directly impact the frequency characteristics of its compositional structure. The gradient parameter ranged from 0.1 to 10, and the stiffness and density of the FGMs beams exhibited significant variations. Therefore, any changes in the gradient parameter substantially impact the first-order natural frequency of the FGMs beams.

The calculation results showed that the Timoshenko beams approached the Euler-Bernoulli beams [26] with a decrease in the height-to-span ratios; the first natural frequencies of the beams increased gradually. For smaller values of h/L, i.e., $h/L = 0.002$ and 0.005, the first natural frequencies of the Timoshenko beams calculated by DQM were very close to the results in the reference. When $p = 0.0001$, it was very close to the first natural frequencies of the Euler-Bernoulli beams made of pure ceramic uniform materials. However, when $p = 10000$, it was very close to the beams made of pure metal

uniform materials. These calculation results proved that DQM was effective and accurate in calculating the natural frequencies of FGMs beams along the thickness direction. The natural frequencies of beams in Figs. 3–5 and the dimensionless natural frequencies of beams were defined as Eq. (40).

$$\Omega = \sqrt{\lambda} = \sqrt{\frac{\rho_m A L^4 \omega^2}{E_m I}} \tag{40}$$

The improved DQM in this article can also provide the vibration mode functions corresponding to all frequencies simultaneously. When the height-to-span ratio $h/L = 0.002$ and the gradient parameter $p = 2$, the first three mode functions of the FGMs beam under the C-C, S-S, and C-F boundary conditions are shown in Figs. 6–8.

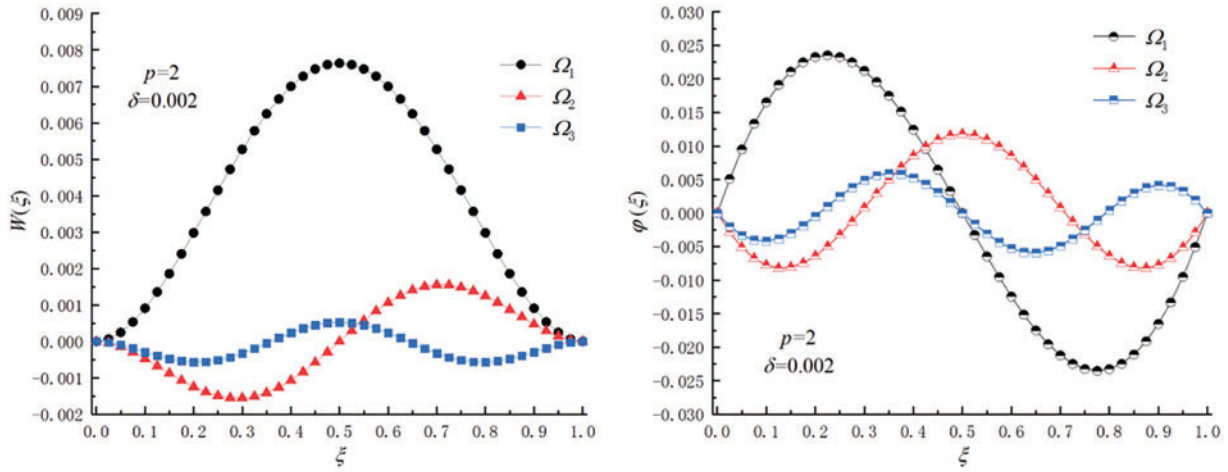

Figure 6: First three orders of modal functions of the beam under C-C boundary condition

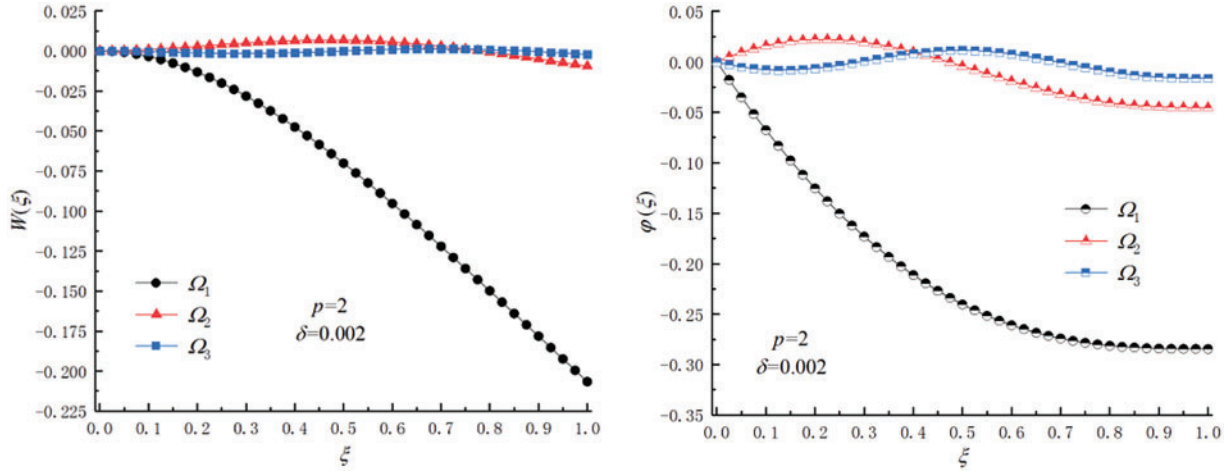

Figure 7: First three orders of modal functions of the beam under C-F boundary condition

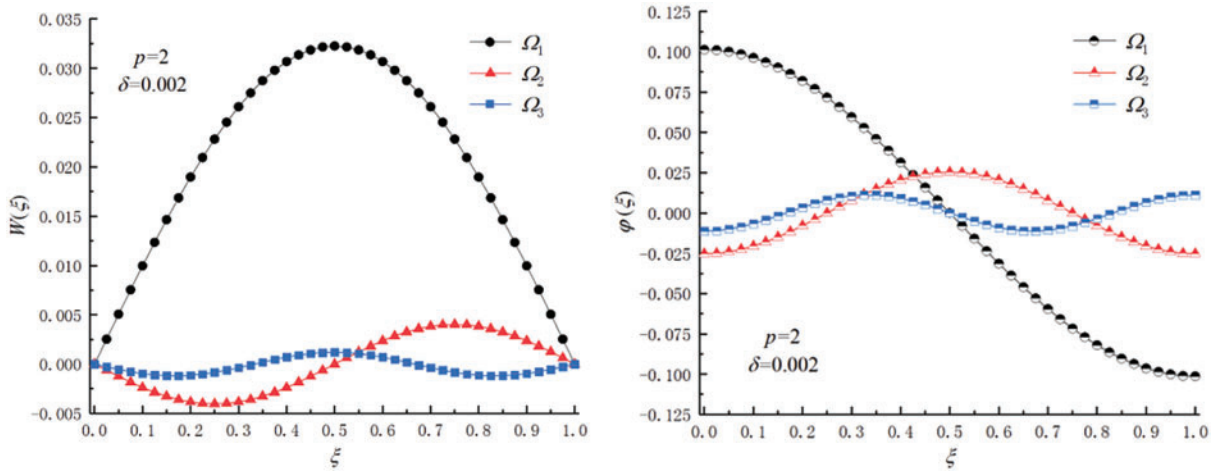

Figure 8: First three orders of modal functions of the beam under S-S boundary condition

3.2 EFM

We also used the finite element method (FEM) based on the ABAQUS software to solve the free vibration of the FGMs Timoshenko beams. Based on the geometric parameters used in the DQM, the length, width, and height of the model of the rectangular cross-sectional beam were 4000 × 200 × 200 mm. Due to the nonlinear characteristics of the beam material, a 3D entity model for the FGMs Timoshenko beam was established by the Matlab program, which was written to define the unit material properties that vary with coordinates. Then, various boundary conditions for frequency analysis and other processes were defined. The eigenfrequency in the ABAQUS software was employed to calculate the first-order frequencies of the FGMs beam. Fig. 9 shows the FEM results of the first natural frequency of an FGMs C-C beam. In the simulation procedure, the material properties are shown in Table 1. The calculated results are listed in Tables 10–12.

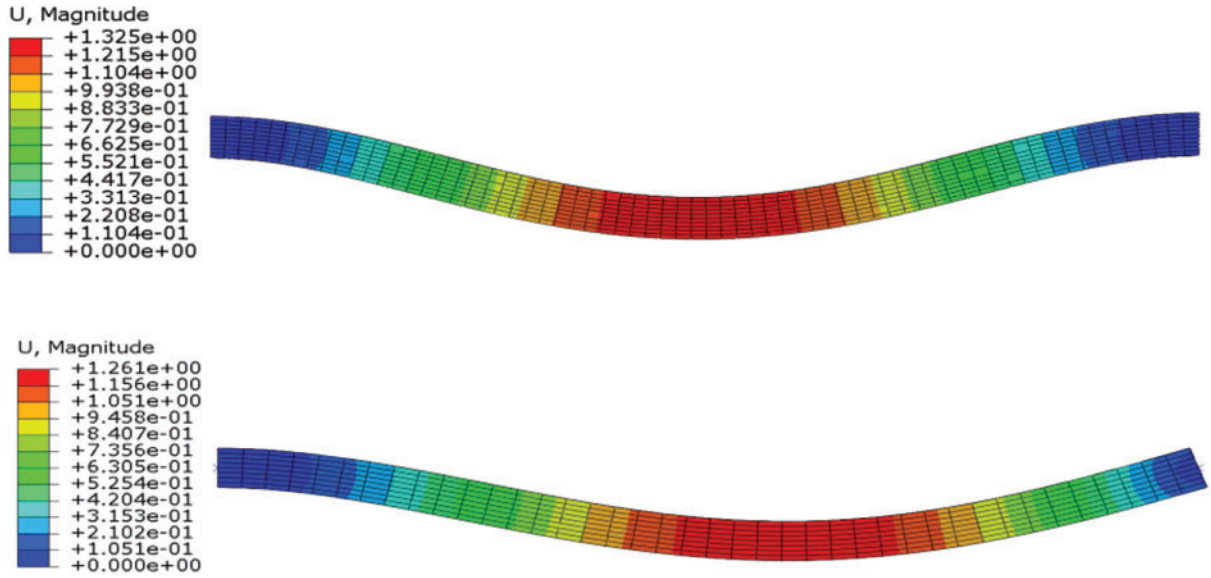

Figure 9: (Continued)

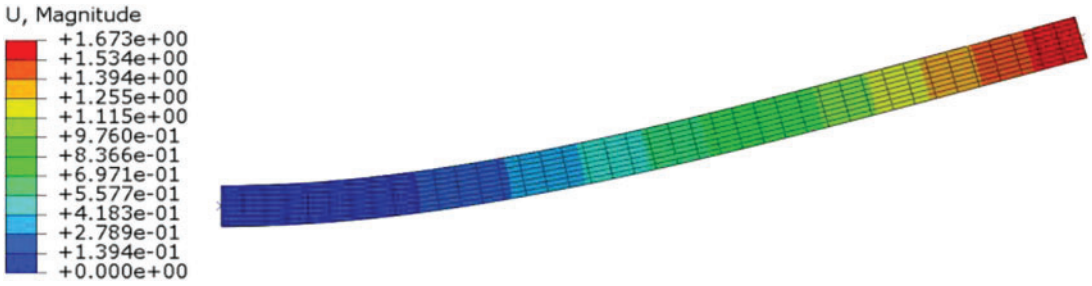

Figure 9: First natural frequency of the FGMs Timoshenko beams with different boundary conditions by the FEM

Table 10: First natural frequencies Ω_1 of functionally graded C-S beam by a different method

BC	δ		p							
			0	1	3	5	7	10	100	∞
C-S	0.2	DQM	47.436	26.025	20.966	19.756	19.089	18.424	15.686	15.130
		EFM	44.564	22.357	17.589	16.895	16.785	15.678	12.357	12.782
	0.05	DQM	48.280	26.453	21.296	20.069	19.396	18.726	15.962	15.399
		EFM	47.649	27.107	21.784	19.687	19.756	18.897	15.664	15.185
	0.01	DQM	48.336	26.481	21.317	20.090	19.416	18.745	15.980	15.417
		EFM	47.895	27.012	20.998	19.247	19.689	19.021	16.124	15.689
	Ref. [23]		48.341	26.483	21.319	20.091	19.418	18.747	15.981	15.418

Table 11: First natural frequencies Ω_1 of functionally graded C-C beam by a different method

BC	δ		p							
			0	1	3	5	7	10	100	∞
C-C	0.2	DQM	68.747	37.721	30.390	28.635	27.669	26.704	22.733	21.927
		EFM	60.214	32.688	21.578	20.687	20.314	19.354	15.247	14.254
	0.05	DQM	70.054	38.383	30.900	29.121	28.144	27.171	23.160	22.344
		EFM	69.855	38.926	31.245	28.954	27.896	27.224	23.478	21.966
	0.01	DQM	70.140	38.426	30.93	29.152	28.175	27.201	23.188	22.372
		EFM	69.856	37.754	29.654	28.754	27.689	26.414	22.879	21.874
	Ref. [23]		70.147	38.429	30.935	29.154	28.177	27.203	23.189	22.373

Table 12: First natural frequencies Ω_1 of functionally graded C-F beam by a different method

BC	δ		p							
			0	1	3	5	7	10	100	∞
C-F	0.2	DQM	11.039	6.047	4.867	4.587	4.433	4.280	3.649	3.521
		EFM	10.956	6.045	4.124	4.321	4.214	4.214	3.552	3.245
	0.05	DQM	11.024	6.039	4.861	4.581	4.428	4.275	3.644	3.516
		EFM	10.939	6.362	4.578	4.321	4.326	4.356	3.558	3.483
	0.01	DQM	11.023	6.039	4.861	4.581	4.428	4.275	3.644	3.516
		EFM	10.956	5.978	4.687	4.547	4.478	4.124	3.541	3.412
	Ref. [23]		11.024	6.039	4.861	4.581	4.428	4.275	3.644	3.516

Tables 10–12 show that the first natural frequency has errors or even distortions with EFM when the boundary conditions are fixed support and simple support with a length-to-height ratio of 0.2. However, under other length-to-height ratios and boundary conditions, the results of EFM are closer to those of DQM and literature results, especially when the length-to-height ratio is relatively large, showing excellent consistency with the results in the literature [23] and those of DQM. This further indicates that the applicability of the Differential Quadrature Method for calculating the natural frequencies of FGMs beams is better than that of the Finite Element Method for short, thick beams.

4 Conclusion

This study investigates the dynamic natural characteristics of FGMs Timoshenko beams using the improved Differential Quadrature Method. Firstly, based on the first-order shear deformation theory, the governing equation of transverse free vibration of an FGMs beam is transformed into the eigenvalue problem of ordinary differential equations. Finally, the QR method can calculate the first several natural frequencies of transverse free vibration of an FGMs beam. In conjunction with the results reported in related literature, the Finite Element Method was introduced to verify the feasibility and accuracy of the developed Differential Quadrature Method. The main conclusions are as follows:

(1) The natural frequencies of the FGMs Timoshenko beams were calculated using improved DQM and EFM. The numerical results showed excellent consistency with those obtained in the reference. The applicability and high efficiency of the proposed method for calculating the natural frequencies of FGMs Timoshenko beams were proved.

(2) The shear deformation and rotational inertia of the FGMs beams' cross-section influence the natural frequency. For smaller values of h/L, i.e., $h/L = 0.002$ and 0.005, the relations between the non-dimensional frequency parameter and frequency order were almost linear. The relations became nonlinear with the increase of height-to-span ratios, and the first natural frequency of the beam increases with a decreasing height-span ratio.

(3) The effects of shear deformation and rotational inertia on the natural frequencies of the FGMs beams cannot be neglected when the beams have relatively large height-span ratios (such as $h/L = 0.2$ and $h/L = 0.1$).

Acknowledgement: I express my gratitude to Anhui Polytechnic University and Hohai University for administrative and technical support.

Funding Statement: Anhui Provincial Natural Science Foundation (2308085QD124), Anhui Province University Natural Science Research Project (Grant No. 2023AH050918). The University Outstanding Youth Talent Support Program of Anhui Province.

Author Contributions: The authors confirm their contribution to the paper as follows: study conception and design: Xiaojun Huang, Liaojun Zhang; data collection: Hanbo Cui; analysis and interpretation of results: Hanbo Cui; draft manuscript preparation: Hanbo Cui, Gaoxin Hu. All authors reviewed the results and approved the final version of the manuscript.

Availability of Data and Materials: The authors confirm that the data supporting the findings of this study are available within the article.

Conflicts of Interest: The authors declare that they have no conflicts of interest to report regarding the present study.

References

1. Kirlangic, O., Akbas, S. D. (2021). Dynamic responses of functionally graded and layered composite beams. *Smart Structures and Systems, 27(1),* 115–122.
2. Shang Hsu, Y. (2016). Enriched finite element methods for Timoshenko beam free vibration analysis. *Applied Mathematical Modelling, 40(15),* 7012–7033.
3. Moallemi-Oreh, A., Karkon, M. (2013). Finite element formulation for stability and free vibration analysis of timoshenko beam. *Advances in Acoustics and Vibration, 2(1),* 1–7.
4. Xu, S., Wang, X. (2011). Free vibration analyses of Timoshenko beams with free edges by using the discrete singular convolution. *Advances in Engineering Software, 42(6),* 797–806.
5. Sorrentino, S., Fasana, A., Marchesiello, S. (2007). Analysis of non-homogeneous Timoshenko beams with generalized damping distributions. *Journal of Sound and Vibration, 304(3–5),* 779–792.
6. Rajasekaran, S., Norouzzadeh Tochaei, E. (2014). Free vibration analysis of axially functionally graded tapered Timoshenko beams using differential transformation element method and differential quadrature element method of lowest-orde. *Meccanica, 49(3),* 995–1009.
7. Shahba, A., Attarnejad, R., Tavanaie Marvi, M., Hajilar, S. (2011). Free vibration and stability analysis of axially functionally graded tapered Timoshenko beams with classical and non-classical boundary conditions. *Composites Part B: Engineering, 42(4),* 801–808. https://doi.org/10.1016/j.compositesb.2011.01.017
8. Sankar, B. V. (2001). An elasticity solution for functionally graded beams. *Composites Science & Technology, 61(5),* 689–696. https://doi.org/10.1016/S0266-3538(01)00007-0
9. Pu, Y., Jia, S., Luo, Y., Shi, S. (2023). Bending analysis of functionally graded sandwich beams with general boundary conditions using a modified Fourier series method. *Archive of Applied Mechanics, 93(2),* 3741–3760.
10. Stojanovic, V., Petkovic, M. D., Deng, J. (2019). Stability and vibrations of an overcritical speed moving multiple discrete oscillators along an infinite continuous structure. *European Journal of Mechanics-A/Solids, 75(1),* 367–380.
11. Stojanovic, V., Petkovic, M. D., Deng, J. (2019). Stability of parametric vibrations of an isolated symmetric cross-ply laminated plate. *Composites Part B: Engineering, 167,* 631–642. https://doi.org/10.1016/j.compositesb.2019.02.041

12. Qian, L. F., Ching, H. K. (2004). Static and dynamic analysis of 2D functionally graded elasticity by using meshless local Petrov-Galerkin method. *Journal of the Chinese Institute of Engineers, 27(4),* 491–503. https://doi.org/10.1080/02533839.2004.9670899
13. Xiang, H. J., Yang, J. (2008). Free and forced vibration of a laminated FGM Timoshenko beam of variable thickness under heat conduction. *Composites Part B: Engineering, 39(2),* 292–303. https://doi.org/10.1016/j.compositesb.2007.01.005
14. Gao, Y., Xiao, W. S., Zhu, H. (2019). Nonlinear vibration analysis of different types of functionally graded beams using nonlocal strain gradient theory and a two-step perturbation method. *European Physical Journal Plus, 134(1),* 1–24.
15. Gao, Y., Xiao, W. S., Zhu, H. (2019). Nonlinear vibration of functionally graded nano-tubes using nonlocal strain gradient theory and a two-steps perturbation method. *Structural Engineering & Mechanics, 69(2),* 205–219.
16. Gao, Y., Xiao, W. S., Zhu, H. (2020). Snap-buckling of functionally graded multilayer graphene platelet-reinforced composite curved nanobeams with geometrical imperfection. *European Journal of Mechanics-A/Solids, 82(5),* 103993–103993.
17. Stojanovic, V., Kozic, P., Ristic, M. (2015). Vibrations and stability analysis of multiple rectangular plates coupled with elastic layers based on different plate theories. *International Journal of Mechanical Sciences, 92(1),* 233–244.
18. Zheng, Z., Tao, Y. (2007). Analytical solution of a cantilever functionally graded beam. *Composites Science and Technology, 67(3–4),* 481–488.
19. Huang, X., Zhang, L., Ge, R., Cui, H., Xu, Z. (2022). Investigation of the free vibrations of radial functionally graded circular cylindrical beams based on differential quadrature method. *Computer Modeling in Engineering & Sciences, 132(3),* 23–41. https://doi.org/10.32604/cmes.2022.019765
20. Huang, X., Zhang, L., Ge, R., Cui, H. (2023). Investigation of the free vibrations of bi-directional functionally graded material beams using differential quadrature method. *Journal of Vibration and Control, 1(3),* 95–104.
21. Choe, H. U., Zhang, J. B., Kim, W., Rim, H., Kim, H. (2023). Free vibration analysis of functionally graded straight-curved-straight beam with general boundary conditions. *Journal of Vibration Engineering & Technologies, 5(4),* 112–131.
22. Patil, M. A., Kadoli, R. (2023). Analytical solution for free vibration of symmetric Terfenol-D layered functionally graded beam with different boundary conditions. *Journal of the Brazilian Society of Mechanical Sciences and Engineering, 45(7),* 357–328.
23. ShiRong, L., Ping, L., Similar transformation between static and dynamic solutions of functionally graded beams and homogeneous beams. *Mechanics in Engineering, 32(2),* 45–49.
24. Sina, S. A., Navazi, H. M., Haddadpour, H. (2009). An analytical method for free vibration analysis of functionally graded beams. *Materials and Design, 30(3),* 741–747. https://doi.org/10.1016/j.matdes.2008.05.015
25. Imek, M. (2010). Fundamental frequency analysis of functionally graded beams by using different higher-order beam theories. *Nuclear Engineering and Design, 240(4),* 697–705. https://doi.org/10.1016/j.nucengdes.2009.12.013
26. Li, S. R., Cao, D. F., Wan, Z. Q. (2013). Bending solutions of FGM Timoshenko beams from those of the homogenous Euler-Bernoulli beams. *Applied Mathematical Modelling, 37(10–11),* 7077–7085.